

Four-wheel steer control corresponding to change in road surface condition by sliding mode control

Misawa Kasahara ¹

Abstract: According to the National Police Agency, there has been an increase in the number of automobile crash victims, making it crucial to manufacture vehicles that anybody can drive safely. However, even if such vehicles are available, individuals may still drive dangerously, so methods of reducing driver overconfidence have become necessary. The road surface conditions on the right side of a vehicle may differ from those on the left, and if a vehicle is moving too fast, it may spin out of control. In this study, we investigate trajectory tracking control for four-wheeled vehicles using our proposed sliding-mode control method.

keywords: Vehicle model, Road conditions

1 Introduction

People ranging in age from the teen years to, over 65 are, regularly on the road driving vehicles. Unfortunately, accidents involving elderly drivers are occurring more and more frequently. It is a difficult situation because the elderly require a vehicle for daily errands, such as shopping, or going to the hospital, particularly, in more rural areas where there is little or no public transportation. Therefore, it is necessary to manufacture safe vehicles that anyone can drive.

Various control algorithms have been proposed for lane-keeping control [1]. It is common to set the control-standard point of a vehicle as the center of gravity. However, this point may be the center of percussion of either the front or the rear wheels. The center of percussion (front virtual point) of the rear wheels is at the point where lateral acceleration is not affected, even if lateral force acts on the rear wheels, and the center of percussion (rear virtual point) of the front wheels is the point where lateral acceleration is not affected, even if lateral force acts on the front wheels. By using these virtual points, the side slip angles can be easily obtained. Several studies using a virtual point as the control-standard point have been done.

Lane-keeping control of the front virtual point maintains an objective trajectory using a sliding mode controller[2, 3]. These are lane-keeping con-

trols only at one point. Even if the objective trajectory is maintained at one side of the vehicle, both of the wheels on that side may not maintain an objective trajectory.

Studies for setting up the front and rear virtual points have been conducted to solve the problem mentioned above. Two lane-keeping control methods for the two virtual points are the automatic steering method that uses all state feedback[4], and the sliding mode controller [5, 6]. Raksincharoensak et al. [4] did not consider disturbance, such as side wind and variations in cornering power, while, Hiroka et al. [5], [6] did take these disturbances into consideration. All three studies took the relation between the steering angles of the front and rear wheels into account. When the rear wheels have been greatly steered from front wheels, it is difficult to maintain an objective trajectory. Furthermore, the driver will be exposed to danger by the protrusion of the spinning wheel outside the lane. Even if a completely safe vehicle is available, an individual may still drive dangerously.

We previously designed a sliding mode controller using a simple two-wheeled model [7]. With this model, we assumed that all four wheels of a vehicle run on the same road surface condition. However, when drivers change lanes, they encounter unexpected situations such as the wheels sliding on only one side, if a vehicle's speed is too fast. Therefore, it is necessary to design a new vehicle model.

¹Robot Engineering Course, Monozukuri Department, Tokyo Metropolitan College of Industrial Technology

2 Vehicle Model

2.1 Road Condition

As shown in Fig. 1, the road surface conditions of a lane are never uniform. For example, a wheel on one side may go through a puddle, the road surface may be frozen, or there may be slick railroad tracks running across the road. If the vehicle is moving too fast, it may spin out of control. Mistakes in a driver's judgment under such conditions may lead to serious accidents. Therefore, the aim of our method is to construct controllers for four-wheeled vehicles to ensure safe driving, even under changing road surface conditions.

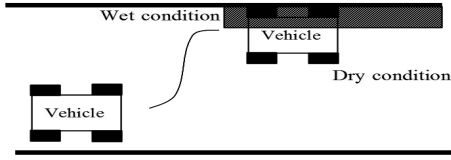


Fig 1: Road Condition

2.2 Four-wheeled Vehicle Model

A model of a four-wheeled vehicle is shown in Fig. 2, and a wheel model is shown in Fig. 3.

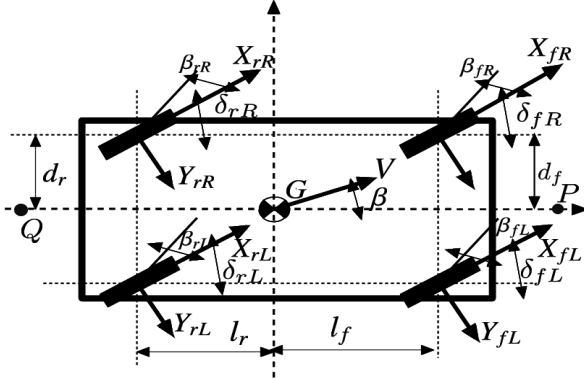


Fig 2: 4ws vehicle model

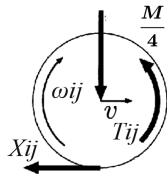


Fig 3: Tire model

I is moment of inertia, m is vehicle mass, β is side slip corner of vehicle, γ is yaw rate. X_{fl} , X_{fr} , X_{rl} , X_{rr} are front left, front right, rear left, and rear right longitudinal forces, respectively, Y_{fl} , Y_{fr} , Y_{rl} , Y_{rr} are front left, front right, rear left, and rear right lateral forces, respectively. l_f is distance from center of gravity to front axles, l_r is distance from center of gravity to rear axles, $l (= l_f + l_r)$ is wheel base, l_w is distance from center of gravity to agitation point of action. δ_{fl} , δ_{fr} , δ_{rl} , δ_{rr} are front left, front right, rear left, and rear right steering angles, respectively. G is center of gravity, w is agitation such as side winds in which vehicle speed is maintained perpendicularly, V [m/s] is speed of vehicle to ground, ω_{ij} ($i = r$ or l , $j = r$ or l) [rad/s] is angular velocity. μ [Nm - s/rad] is axle friction, R [m] is wheel radius, I_i ($i = r$ or l) [kgm²] are wheel moment of inertia for front and rear. T_{ij} ($i = r$ or l , $j = r$ or l) [Nm] are brake torque for front left, front right, rear left, and rear right, respectively.

The equation of motion of a car is derived using the models shown in Figs. 2 and 3.

Equation of longitudinal direction motion :

$$m(\dot{u} - v\gamma) = X_{fr} + X_{fl} + X_{re} + X_{rl} \quad (1)$$

Equation of transverse direction motion :

$$m(\dot{v} + u\gamma) = Y_{fr} + Y_{fl} + Y_{rr} + Y_{rl} + w \quad (2)$$

Equation of yaw motion :

$$I\dot{\gamma} = l_f(Y_{fr} + Y_{fl}) - l_r(Y_{rr} + Y_{rl}) - l_w w + N \quad (3)$$

Equation of yaw moment

$$N = \frac{d_f}{2}(X_{fr} - X_{fl}) + \frac{d_r}{2}(X_{rr} - X_{rl}) \quad (4)$$

Equation of rotary motion

$$I_w \dot{\omega}_{ij} = -R X_{ij} + T_{ij} \quad i = f \text{ or } r, j = r \text{ or } l \quad (5)$$

2.3 Vehicle Speed

Since the speed in the direction of movement is usually fast enough compared with that in the direction of order, it can be assumed that it is $|\beta| \ll 1$.

$$u = V \cos \beta \approx V \quad (6)$$

$$v = V \sin \beta \approx V\beta \quad (7)$$

$$\dot{u} = \dot{V} \cos \beta - V \sin \beta \dot{\beta} \approx \dot{V} - V\beta \dot{\beta} \quad (8)$$

$$\dot{v} = \dot{V} \sin \beta + V \cos \beta \dot{\beta} \approx \dot{V}\beta + V\dot{\beta} \quad (9)$$

2.4 Cornering Forces

$Y_{fj}, Y_{rj} (j = l, r)$, which are the cornering forces of the front and rear, are expressed by the following equations, where $K_{fj}, K_{rj} (j = l \text{ or } r)$ are the cornering coefficients of the front and rear, respectively.

$$Y_{fj} = -K_{fj}\beta_{fj} = -K_{fj}\left(\beta + \frac{l_f\gamma}{V} - u_{fj}\right) \quad (10)$$

$$Y_{rj} = -K_{rj}\beta_{rj} = -K_{rj}\left(\beta - \frac{l_r\gamma}{V} - u_{rj}\right) \quad (11)$$

2.5 Equation-of-State Model of the Vehicle

The motion equations of the linear vehicle model are derived, where $x = [\beta \ \gamma]^T$ is a state vector. The equation-of-state vehicle model is expressed by the following equation.

$$\dot{x} = Ax + B_1u_1 + B_2u_2 + C_1w + C_2N \quad (12)$$

$$u_1 = [u_{fl} \ u_{fr}]^T, \quad u_2 = [u_{rl} \ u_{rr}]^T$$

$$A = \begin{bmatrix} A_{11} & A_{12} \\ A_{21} & A_{22} \end{bmatrix}$$

$$A_{11} = -\frac{\dot{v}}{v} - \frac{K_{fl} + K_{fr} + K_{rl} + K_{rr}}{mv}$$

$$A_{12} = -1 - \frac{(K_{fl} + K_{fr})l_f - (K_{rl} + K_{rr})l_r}{mv^2}$$

$$A_{21} = -\frac{(K_{fl} + K_{fr})l_f - (K_{rl} + K_{rr})l_r}{I}$$

$$A_{22} = -\frac{(K_{fl} + K_{fr})l_f^2 + (K_{rl} + K_{rr})l_r^2}{Iv}$$

$$B_1 = \begin{bmatrix} \frac{K_{fl}}{mv} & \frac{K_{fr}}{mv} \\ \frac{K_{fl}l_f}{I} & \frac{K_{fr}l_f}{I} \end{bmatrix}, \quad B_2 = \begin{bmatrix} \frac{K_{rl}}{mv} & \frac{K_{rr}}{mv} \\ -\frac{K_{rl}l_r}{I} & -\frac{K_{rr}l_r}{I} \end{bmatrix}$$

$$u_1 = [u_{fl} \ u_{fr}]^T, \quad u_2 = [u_{rl} \ u_{rr}]^T$$

$$C_1 = \begin{bmatrix} \frac{1}{mv} & -\frac{l_w}{I} \end{bmatrix}^T, \quad C_2 = \begin{bmatrix} 0 & \frac{1}{I} \end{bmatrix}^T$$

3 Trajectory Deviation System

3.1 Definition of Control Threshold

The center of percussion of the rear wheels (front virtual point) is at the front control standard point P[6], while, the center of percussion of the front wheels (rear virtual point) is at the rear control

standard point Q.

$$L_p = \frac{I}{ml_r}, \quad L_q = \frac{I}{ml_f} \quad (13)$$

Therefore, the reference points of lane location is set as P and Q.

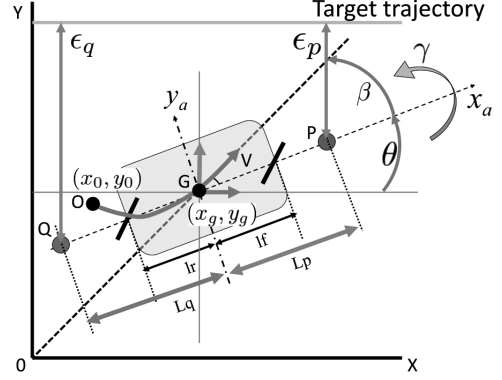


Fig 4: Vehicle model on ground

3.2 Trajectory Deviation System of Temporal Differentiation

For the maintenance of the traffic lane by the steering, we think about the case that fixed a vehicle to show in Fig. 4 on the ground. The trajectory deflection $\epsilon_p \ \epsilon_q$ of the objective trajectory of the front and rear control-standard points and actual running trajectory are expressed by the following equation.

$$\left. \begin{aligned} \epsilon_p &= z_p - y_p \\ \epsilon_q &= z_q - y_q \end{aligned} \right\} \quad (14)$$

y_p, y_q is the distance in the y axial direction of the running trajectory of the front and rear control thresholds and z_p, z_q is the distance in the y axial direction between the reference trajectories of the front and rear control thresholds (y axis). The target position can be maintained by having the trajectory deflection equal zero. Therefore, if we assume a position for a coordinate system fixed by the ground (x_g, y_g) , and we can obtain the yaw angle for the x axis of the vehicle with θ . y_0 is an initial value of the distance of the y axial direction. The distance of the y axial direction of the front and rear control thresholds

$P = (x_p, y_p)$, $Q = (x_q, y_q)$ is expressed by the following equations.

$$\left. \begin{aligned} y_p &= v \int_0^t \sin(\beta + \theta) d\tau + y_0 + L_p \sin \theta \\ y_q &= v \int_0^t \sin(\beta + \theta) d\tau + y_0 - L_q \sin \theta \end{aligned} \right\} \quad (15)$$

Therefore, trajectory deflection of the front and rear wheels, ϵ_p, ϵ_q are expressed as following equations.

$$\epsilon_p = -v \int_0^t \sin(\beta + \theta) d\tau - y_0 - L_p \sin \theta + z_p \quad (16)$$

$$\epsilon_q = -v \int_0^t \sin(\beta + \theta) d\tau - y_0 + L_q \sin \theta + z_q \quad (17)$$

θ_0 is the initial value of the yaw angle θ , and its differentiations are $\theta = \theta_0 + \int_0^t \gamma d\tau$, $\dot{\theta} = \gamma$. Therefore, the temporal differentiation of Eq. (17) is expressed as following equations.

$$\left. \begin{aligned} \dot{\epsilon}_p &= -\{v(\beta + \theta) + L_p \gamma\} \\ \dot{\epsilon}_q &= -\{v(\beta + \theta) - L_q \gamma\} \end{aligned} \right\} \quad (18)$$

From Eq. (18), the state vector $x = [\beta \ \gamma]^T$ is expressed as following equations.

$$x = T\dot{\epsilon} + vT\theta \quad (19)$$

$$T = \frac{1}{v(L_p + L_q)} \begin{bmatrix} -L_q & -L_p \\ -v & v \end{bmatrix} \quad (20)$$

$$\dot{\epsilon} = [\dot{\epsilon}_p \ \dot{\epsilon}_q]^T.$$

The results of carrying out time differentiation using Eq.(19) are shown below.

$$\ddot{\epsilon} = T_1 \dot{x} + T_2 x - \dot{v}T_3 \theta \quad (21)$$

$$T_1 = \begin{bmatrix} -v & -L_p \\ -v & L_q \end{bmatrix}, T_2 = \begin{bmatrix} -\dot{v} & -v \\ -\dot{v} & -v \end{bmatrix}, T_3 = \begin{bmatrix} 1 \\ 1 \end{bmatrix}$$

3.3 Steering Angles

We investigated a trajectory tracking controller for four-wheeled vehicles. We built a vehicle model in which the road surface conditions differed on either side of the vehicle, and derived an analysis model corresponding to the change in speed or road conditions. Speed, road conditions, side wind, etc. were all robust. When a driver turns a vehicle's wheels, the steering angles are determined in accordance with this turn. When the right and left road surfaces differ, vehicles may slip. As a result, the trajectory where it actually runs shifts more than the reference trajectory. And, slipping

becomes a cause of the accident. If the front and rear wheels are steered like a snowplow's, the vehicle will stop effectively. Therefore, when a vehicle is likely to slip, we can derive a controller that steers a wheel like a snowplow's without interfering with a driver's steering.

We derived a trajectory tracking controller using sliding-mode control, and performed a numeric simulation to evaluate its effectiveness.

When the conventional controller was used, the front and rear wheels swerved from the trajectory, while, when the proposed trajectory controller was used, the front and rear wheels ran along the trajectory. This clearly demonstrates the effectiveness of the proposed method. In the future, we intend to design optimal steering angles such as the snowplow angle to theoretically clarify the advantages of the proposed technique.

Usually, drivers operate a handle and the steering angle changes based upon this. It is therefore also necessary to take the driver's steering into account. To design safe vehicles, we need a controller that takes into account driver operation. In the future, we will investigate driver's operation of front wheels.

Under normal conditions :

$$u_{fl} = u_f \quad (22)$$

$$u_{fr} = u_f = flag * u_f \quad flag = 1 \quad (23)$$

In an emergency

$$u_{rl} = u_r \quad (24)$$

$$u_{rr} = -u_r = flag * u_r \quad flag = -1 \quad (25)$$

Substituting Eqs.(22), (23), (24) and (25) into Eq.(12), we obtain the following equations.

$$\dot{x} = A_A x + B_B u + C_1 w + C_2 N \quad (26)$$

$$u = [u_f \ u_r]^T \quad (27)$$

$$A_A = \begin{bmatrix} A_{A11} & A_{A12} \\ A_{A21} & A_{A22} \end{bmatrix} B_B = \begin{bmatrix} \frac{K_f}{mv} & \frac{K_r}{mv} \\ \frac{K_{fl}}{I} & \frac{K_{rl}}{I} \end{bmatrix}$$

$$C_1 = \begin{bmatrix} \frac{1}{mv} & \frac{-l_w}{I} \end{bmatrix}^T, C_2 = \begin{bmatrix} 0 & \frac{1}{I} \end{bmatrix}^T$$

$$A_{A11} = -\frac{K_{fl} + K_{fr} + K_{rl} + K_{rr}}{mv}$$

$$\begin{aligned}
A_{A12} &= -1 - \frac{(K_{fl} + K_{fr})l_f - (K_{rl} + K_{rr})l_r}{mv^2} \\
A_{A21} &= -\frac{(K_{fl} + K_{fr})l_f - (K_{rl} + K_{rr})l_r}{I} \\
A_{A22} &= -\frac{(K_{fl} + K_{fr})l_f^2 + (K_{rl} + K_{rr})l_r^2}{Iv} \\
K_f &= K_{fl} + flag * K_{fr} \\
K_r &= K_{rl} + flag * K_{rr}
\end{aligned}$$

3.4 Derivation of the State Equations

The purpose of our study is to have the trajectory deflection equal zero. Substituting Eqs. (12) and (19) into Eq. (21) yields Eq. (28).

$$\begin{aligned}
\ddot{e} &= A_e(T\dot{e} + v\theta) + B_e u + C_{e1}w + C_{e2}N - \dot{v}T_3\theta \quad (28) \\
A_e &= \begin{bmatrix} \frac{K_{fl}}{ml_r} & \frac{K_{fl}l_f}{ml_r V} \\ \frac{K_{rl}}{ml_f} & -\frac{K_{rl}l_r}{ml_f v} \end{bmatrix}, B_e = \begin{bmatrix} -\frac{K_{fl}}{ml_r} & 0 \\ 0 & -\frac{K_{rl}}{ml_f} \end{bmatrix} \\
C_{e1} &= \begin{bmatrix} -\frac{l_r - l_w}{ml_f} \\ \frac{ml_r}{l_f + l_w} \end{bmatrix}, C_{e2} = \begin{bmatrix} -\frac{1}{ml_r} \\ \frac{1}{ml_f} \end{bmatrix}
\end{aligned}$$

We receive feedback from Eq.(29).

$$u = \bar{u} + K(\dot{e} + v\theta - (A_e T)^{-1}\dot{v}\theta) \quad (29)$$

Substituting Eq. (28) into Eq. (29), we obtain the following, where $\bar{u} = [\bar{u}_f \ \bar{u}_r]^T$.

$$\begin{aligned}
\ddot{e} &= (A_e T + B_e K)(\dot{e} + v\theta) - B_e K(A_e T)^{-1}\dot{v}\theta - \dot{v}\theta \\
&\quad + B_e \bar{u} + C_{e1}w + C_{e2}N \quad (30)
\end{aligned}$$

K is defined as $K = -B_e^{-1}A_e T$. As a result $A_e T + B_e K = 0$ and the effect of θ can be ignored. Therefore,

$$\ddot{e} = B_e \bar{u} + C_{e1}w + C_{e2}N. \quad (31)$$

4 Sliding Mode Control

We developed a controller to have a front trajectory deviation equal to zero using the sliding mode control method. Similarly, we developed a controller to have a rear wheel trajectory deviation equal to zero by using the same method.

4.1 Design of Controller for Front Trajectory Deviation

A state equation of the front trajectory deviation is expressed by Eq.(32).

$$\begin{aligned}
\begin{bmatrix} \dot{\epsilon}_p \\ \dot{\epsilon}_p \end{bmatrix} &= \begin{bmatrix} 0 & 1 \\ 0 & 0 \end{bmatrix} \begin{bmatrix} \epsilon_p \\ \dot{\epsilon}_p \end{bmatrix} + \begin{bmatrix} 0 \\ -\frac{K_{fl}}{ml_r} \end{bmatrix} \bar{u}_f \\
&\quad + \begin{bmatrix} 0 \\ -\frac{l_r - l_w}{ml_r} \end{bmatrix} w + \begin{bmatrix} 0 \\ -\frac{1}{ml_r} \end{bmatrix} N \\
&= A_{pq} \begin{bmatrix} \epsilon_p \\ \dot{\epsilon}_p \end{bmatrix} + B_p \bar{u}_f + C_{p1}w + C_{p2}N \\
&= A_{pq} \begin{bmatrix} \epsilon_p \\ \dot{\epsilon}_p \end{bmatrix} + \begin{bmatrix} 0 \\ -\frac{K_{fl}}{ml_r} \end{bmatrix} (\bar{u}_f + d_p) \quad (32)
\end{aligned}$$

$$d_p = \frac{l_r - l_w}{K_{fl}} w + \frac{1}{K_{fl}} N \quad (33)$$

A switching function σ_p of the front trajectory deviation is expressed by Eq. (34):

$$\sigma_p = S_p \begin{bmatrix} \epsilon_p \\ \dot{\epsilon}_p \end{bmatrix} = [S_{p1} \ S_{p2}] \begin{bmatrix} \epsilon_p \\ \dot{\epsilon}_p \end{bmatrix} \quad (34)$$

Control input \bar{u}_f is the sum of the equivalent control input $\bar{u}_{f_{eq}}$ and the nonlinear input $\bar{u}_{f_{nl}}$.

$$\bar{u}_f = \bar{u}_{f_{eq}} + \bar{u}_{f_{nl}} \quad (35)$$

The equivalent control input $\bar{u}_{f_{eq}}$ is expressed by Eq. (36).

$$\bar{u}_{f_{eq}} = -(S_p B_p)^{-1} S_p A_p \begin{bmatrix} \epsilon_p \\ \dot{\epsilon}_p \end{bmatrix} = -\frac{S_{p1}}{S_{p2} B_{p02}} \dot{\epsilon}_p \quad (36)$$

where B_{p02} is defined by the following equation.

$$B_{p02} = -\frac{K_{fl}}{ml_r} \quad (37)$$

In contrast, the nonlinear input $\bar{u}_{f_{nl}}$ is expressed by Eq. (38).

$$\bar{u}_{f_{nl}} = -\rho_p \text{sgn}(\sigma_p) \simeq -\rho_p \frac{\sigma_p}{\|\sigma_p\| + \mu_p} \quad \mu_p > 0 \quad (38)$$

Therefore, the front control input u_f is expressed by Eq. (39) from Eqs. (36), (37), and (38).

$$\bar{u}_f = \bar{u}_{f_{eq}} + \bar{u}_{f_{nl}} = -\frac{S_{p1}}{S_{p2} B_{p02}} \dot{\epsilon}_p - \rho_p \frac{\sigma_p}{\|\sigma_p\| + \mu_p} \quad (39)$$

4.2 Design of Controller for Rear Trajectory Deviation

A state equation of the rear trajectory deviation is expressed by Eq. (40).

$$\begin{aligned} \begin{bmatrix} \dot{\epsilon}_q \\ \ddot{\epsilon}_q \end{bmatrix} &= \begin{bmatrix} 0 & 1 \\ 0 & 0 \end{bmatrix} \begin{bmatrix} \epsilon_q \\ \dot{\epsilon}_q \end{bmatrix} + \begin{bmatrix} 0 \\ -\frac{K_r l}{m l_f} \end{bmatrix} \bar{u}_r \\ &+ \begin{bmatrix} 0 \\ -\frac{l_f + l_w}{m l_f} \end{bmatrix} w + \begin{bmatrix} 0 \\ \frac{1}{m l_f} \end{bmatrix} N \\ &= A_{pq} \begin{bmatrix} \epsilon_q \\ \dot{\epsilon}_q \end{bmatrix} + B_q \bar{u}_r + C_{1q} w + C_{q2} N \\ &= A_{pq} \begin{bmatrix} \epsilon_q \\ \dot{\epsilon}_q \end{bmatrix} + \begin{bmatrix} 0 \\ -\frac{K_r l}{m l_f} \end{bmatrix} (\bar{u}_r + d_q) \end{aligned} \quad (40)$$

$$d_q = \frac{l_f + l_w}{K_r l} w - \frac{1}{K_r l} N \quad (41)$$

A switching function σ_p of the rear trajectory deviation is expressed by Eq. (42).

$$\sigma_q = S_q \begin{bmatrix} \epsilon_q \\ \dot{\epsilon}_q \end{bmatrix} = [S_{q1} \quad S_{q2}] \begin{bmatrix} \epsilon_q \\ \dot{\epsilon}_q \end{bmatrix} \quad (42)$$

Control input \bar{u}_r is the sum of the equivalent control input \bar{u}_{req} and nonlinear input \bar{u}_{rnl} .

$$\bar{u}_r = \bar{u}_{req} + \bar{u}_{rnl} \quad (43)$$

The equivalent control input \bar{u}_{feq} of the rear is expressed by Eq. (44).

$$\bar{u}_{req} = -(S_q B_q)^{-1} S_q A_q \begin{bmatrix} \epsilon_q \\ \dot{\epsilon}_q \end{bmatrix} = -\frac{S_{q1}}{S_{q2} B_{q02}} \dot{\epsilon}_q \quad (44)$$

where B_{p02} is defined by the following equation.

$$B_{q02} = -\frac{K_r l}{m l_f} \quad (45)$$

In contrast, the nonlinear input \bar{u}_{fnl} is expressed by Eq. (46).

$$\begin{aligned} \bar{u}_{rnl} &= -\rho_q \text{sgn}(\sigma_q) \\ &= -\rho_q \frac{\sigma_q}{\|\sigma_q\|} \simeq -\rho_q \frac{\sigma_q}{\|\sigma_q\| + \mu_q}, \quad \mu_q > 0 \end{aligned} \quad (46)$$

Therefore, rear control input u_f is expressed by Eq. (47) from Eqs. (44), (45) and (46).

$$u_r = \bar{u}_{req} + \bar{u}_{rnl} = -\frac{S_{q1}}{S_{q2} B_{q02}} \dot{\epsilon}_q - \rho_q \text{sgn}(\sigma_q) \quad (47)$$

5 Simulation

We performed a simulation in which a vehicle was at the 300m point at start time, and then, the trajectory changed to 310m. The wheels of both sides ran on a dry road surface for 5s after starting. After that, the left wheels ran on a wet surface. The vehicle decelerated upon entering the wet surface. The regular disturbance of side wind was assumed to be 8 ~ 15s. The parameters used in the simulations are listed in Table 1.

When the vehicle slips because turbulence such as the sidewind turbulences and the road changes entered, and it shifts from the reference trajectory, it switches to $flag = -1$.

Table 1: Simulation parameter

m	1300[kg]	v	60[km/h]
l_f	1.0[m]	l_r	1.4[m]
l_w	1.0[m]	w	3000[N]
I	1600[N]		

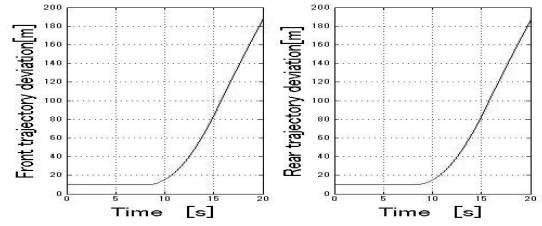


Fig 5: Front-rear trajectory deviation using conventional approach

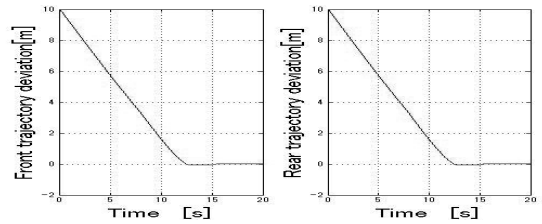


Fig 6: Front-rear trajectory deviation using proposed approach

Fig. 5 shows the results when sliding mode control was carried out using the steering angles ($flag=1$) defined by Eqs. (22) and (23), and Fig. 6 shows those when the angles ($flag=-1$) were defined by Eqs. (24) and (25).

When the conventional control method of making to flag=-1 when seeming to slip was used, the front and rear wheels swerved from the trajectory, while , when the proposed trajectory control method was used, the front and rear wheels maintained the trajectory. This demonstrates the effectiveness of the proposed trajectory control method.

6 Conclusion

We investigated trajectory tracking controller for four-wheeled vehicles. We built a vehicle model in which the road surface conditions differed on either side of the vehicle. We derived an analysis model corresponding to changes in speed or road condition. Speed, road conditions, side wind, etc. were all robust. When a driver turns a vehicle's wheels, the steering angles are determined in accordance with this turn. When the right and left road surfaces differ, a vehicle may slip. If the front and rear wheels are steered like a snowplow's, the vehicle will stop effectively. Therefore, when a vehicle is likely to slip, we can derive a controller that steers the wheel like a snowplow without interfering with the driver's steering.

We developed a trajectory tracking controller using sliding-mode control. We performed a numeric simulation to evaluate its effectiveness.

When the conventional controller was used, the front and rear wheels swerved from the trajectory, while, when the proposed trajectory controller was used, the front and rear wheels ran along the trajectory. This demonstrates the effectiveness of the proposed method. In the future, we intend to design the optimal steering angles like those of a snowplow and to theoretically clarify the advantage of the proposed technique.

Usually, drivers operate a handle and the steering angle changes based upon this. It is therefore also necessary to take the driver's steering into account. To design safe vehicles, we need a controller that takes into account driver operation. In the future, we will investigate drivers operate handle of front wheels. And misgivings to safety by the switch of flag are not examined enough. This respect is assumed to be future tasks.

References

- [1] T. Fujioka, M. Omae , "Overview of Control for Automatic Driving System", *Journal of the Robotics Society of Japan*, Vol.17, No.3, pp. 328–333 (1999)
- [2] H. Kumamoto, I. Sakamoto, K. Tenmoku, H. Shimoura , "Vehicle Steering Control by Reduced-Dimension Sliding Mode Theory and Singular Headway Viewpoint", *Transactions of SICE*, Vol.34, No.5, pp. 393–399 (1998)
- [3] H. Kumamoto, O. Nishihara, K. Tenmoku, H. Shimoura , "Automated, Robust Vehicle Steering on Smoothly Connected Arc Course -Non-Linear, Reduced-Dimension Sliding Mode Controller-", *Transactions of SICE*, Vol.35, No.3, pp. 340–348 (1999)
- [4] P. Raksincharoensak, H. Mouri, M. Nagai , "Three-Dimensional Measurement Using Circular Velocity Bias : Improvement of Measurement Accuracy Using Multi Spot Laser", *Transactions of the Japan Society of Mechanical Engineers. C*, Vol.69, No.681, pp. 1254–1259 (2003)
- [5] T. Hiraoka, O. Nishihara, H. Kumamoto , "Model Following Sliding Mode Control for Active Four-Wheel Steering Vehicle", *Transactions of Society of Automotive Engineers of Japan Transactions of the Society of Automotive Engineers of Japan*, Vol.35, No.4, pp. 163–169 (2004)
- [6] T. Hiraoka, O. Nishihara, H. Kumamoto , "Path Tracking of Four Wheel Steering Vehicle by Using Sliding Mode Control", *Transactions of the Institute of Systems*, Vol.16, No.10, pp. 520–530 (2003)
- [7] M. Kasahara, Y. Kanai, R. Shiraki and Y. Mori, "Adjust Method of Nonlinear Gain in Four-Wheel Steering Control Using Sliding Mode Control", *IEEEJ Transactions on Electronics, Information and Systems*,129(7) , pp.1389-1396 2009